Received: 12 May 2023 | Revised: 14 August 2023 | Accepted: 28 August 2023

DOI: 10.1002/gcc.23200

WILEY

BRIEF REPORT

A novel *HMGA2*::*KITLG* fusion in a dedifferentiated liposarcoma with amplification of *MDM2* and *HMGA2*

Shishan Zhou[1] | Changliang Zhang[2] | Zhipeng Zhang[3] | Yongbin Hu[4,5] | Lina Zhao[2] | Wentao Hu[2] | Si Chen[2] | Bin Li[1] | Sheng Xiao[6]

[1]Department of Oncology, Xiangya Hospital, Central South University, Changsha, China

[2]Suzhou Sano Precision Medicine Ltd, Suzhou, China

[3]Department of Geratology, Xiangya Hospital, Central South University, Changsha, China

[4]Department of Pathology, Xiangya Hospital, Central South University, Changsha, China

[5]Department of Pathology, School of Basic Medical Science, Central South University, Changsha, China

[6]Department of Pathology, Brigham and Women's Hospital, Harvard Medical School, Boston, Massachusetts, USA

Correspondence
Sheng Xiao, Department of Pathology, Brigham and Women's Hospital, Harvard Medical School, 75 Francis Street, Boston, MA 02115, USA.
Email: sxiao@partners.org

Bin Li, Department of Oncology, Xiangya Hospital, Central South University, No.87 Xiangya Road, Changsha, Hunan 410008, China.
Email: bincsuxy@csu.edu.cn

Funding information
Central South University Postgraduate Teaching Case Database Construction Project, Grant/Award Number: 2022ALK039

Abstract

High-mobility group AT-hook 2 (*HMGA2*) is rearranged in various types of mesenchymal tumors, particularly lipomas. *HMGA2* is also co-amplified with mouse double minute 2 (*MDM2*) in well-differentiated liposarcoma/dedifferentiated liposarcoma (WDLPS/DDLPS). We report a case of relapsed DDLPS with a novel in-frame fusion between *HMGA2* and *KITLG*, which encodes the ligand for KIT kinase, a critical protein involved in gametogenesis, hematopoiesis, and melanogenesis. The *HMGA2* breakpoint is in intron 3, a commonly observed location for *HMGA2* rearrangements, while the *KITLG* breakpoint is in intron 2, leading to a fusion protein that contains almost the entire coding sequence of *KITLG*. By immunohistochemical staining, tumor cells expressed KIT and showed phosphorylated MAPK, a major KIT downstream target. We suggest an oncogenic mechanism that involves the overexpression of *KITLG* caused by its rearrangement with *HMGA2*, leading to the constitutive activation of KIT kinase. While *MDM2* amplification was observed in both the primary tumor and the relapsed tumor, the *HMGA2*::*KITLG* was only present in the relapsed tumor, indicating the role of *HMGA2*::*KITLG* in disease progression.

KEYWORDS
HMGA2, *KITLG*, liposarcoma, SCF

1 | INTRODUCTION

Lipoma is a common tumor, and the majority of cases have a straightforward histological diagnosis. However, large, or deep-seated lipomas often require differentiation from well-differentiated liposarcoma, a low-grade malignancy that can progress to high-grade dedifferentiated liposarcoma. Molecular testing of *HMGA2* and *MDM2* can be useful in making this differential diagnosis. Approximately 70% of lipomas exhibit *HMGA2* rearrangement, which is mostly caused by chromosome translocation or inversions. In the remaining lipomas with a normal genome, *HMGA2* is still overexpressed in some cases, suggesting that it plays an important role in these tumors.[1] *MDM2* amplification is a diagnostic marker for well-differentiated liposarcoma/dedifferentiated liposarcoma (WDLPS/DDLPS). Karyotyping analysis typically reveals *MDM2* amplification on ring chromosomes or giant marker chromosomes, which results from complex rearrangements of chromosome 12 via breakage-fusion-bridge cycles. In addition to the karyotype analysis, clinical testing of *MDM2* amplification is often performed using fluorescence in situ hybridization (FISH) with formalin-fixed paraffin-embedded (FFPE) tissue samples.

In this report, we present a case of DDLPS harboring both *MDM2* and *HMGA2* amplification, along with a novel *HMGA2*

Shishan Zhou and Changliang Zhang contributed equally to this study.

fusion. *HMGA2* is frequently co-amplified with *MDM2* in DDLPS, often accompanied by intragenic *HMGA2* rearrangements. Notably, Necchi et al. identified *HMGA2* fusions in 28% of LPS cases, including a *HMGA2::TSFM* fusion in a retroperitoneal DDLPS with pulmonary metastases.[2] In a study by Beird et al., a comparative analysis of genomic and transcriptomic profiles between DDLPS and WDLPS components in 17 patients revealed that DDLPS exhibited higher numbers of somatic copy-number variations, particularly chromosome 12 amplifications, and a greater number of fusions, including *HMGA2* rearrangements with *CCT2*, *FGD6*, *GLB1*, *IGF2*, *KIF21A*, *RP11-74 M13.4*, and *RP11-366L20.2-IGF2*, compared to WDLPS.[3] The oncogenic mechanism of these *HMGA2* fusions in DDLPS is not yet fully understood, but they may collaborate with the MDM2/TP53 pathway to promote tumor cell proliferation and block apoptosis.[3] Also, the HMGA2 fusion partners may contribute to tumorigenesis, as is the case with many other fusion oncogenes in cancer.

2 | MATERIALS AND METHODS

2.1 | Targeted RNA next-generation sequencing

Total RNA from 10-μm FFPE tissue sections were extracted by FFPE Total RNA Miniprep System (Cat: Z1002, Promega, USA). 100 ng of total RNA was used for reverse transcription, end repairing, and adaptor ligation according to standard next-generation sequencing (NGS) protocols (Cat: E7771 and E6111, NEB, USA). PCR enrichment was performed using 555 gene specific primers to detect a group of 99 genes commonly involved in solid tumors (Table S1), and the enriched PCR products were sequenced in an NovaSeq 6000 platform (Illumina, USA). The sequencing data were analyzed with SeqNext software (JSI, Germany).

2.2 | Targeted DNA NGS

Genomic DNA from 10-μm FFPE tissue sections was isolated with FFPE gDNA Miniprep System (Cat: A2351, Promega, USA). 300 ng DNA was fragmented with a Bioruptor Pico (Diagenode, USA) to 200–300 bp, and library preparation was performed using the Rapid Plus DNA Lib Prep Kit for Illumina (RK20208, ABclonal, USA) according to the manufacturer's specifications. The libraries were incubated with a pool of biotin-labeled bait oligos that targeted 638 genes commonly involved in tumors for 16 h, targeted regions were pulled down with streptavidin beads, amplified by PCR, and sequenced as paired-end 150-bp reads on an Illumina NextSeq 6000 instrument. Reads were aligned to the reference genome (hg19) using BWA-MEM. Sequencing results for single-nucleotide variations, insertion/deletion (Indels), copy number variations, and structure variations were analyzed with SeqNext software (JSI, Germany) and laboratory-developed pipelines (Sano Medical Laboratories, China).

2.3 | Fluorescence in situ hybridization

FISH was performed on 5-μm tissue sections with probes for *MDM2* and *HMGA2* (Be true, China). *MDM2* probe (red) is coupled with a centromere 12 control probe (green) and the *HMGA2* split probes consist of 5′ probe (green) and 3′ probe (red). The slides were deparaffinized in Xylene, rehydrated, treated in 750 U/mL pepsin digest solution

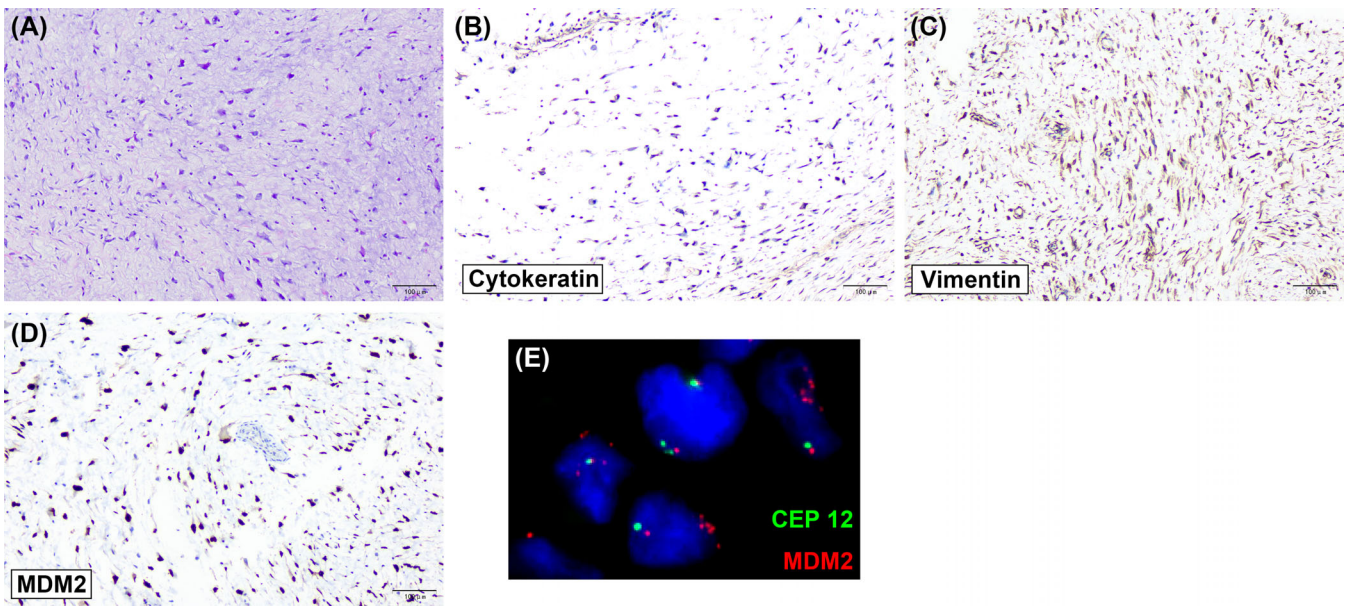

FIGURE 1 H&E staining of the primary tumor tissue sections showed a spindle and pleomorphic tumor (A); IHC was negative for Cytokeratin (B), positive for Vimentin (C), and positive for MDM2 (D); FISH with CEP 12 (green) and MDM2 (red) probes showed MDM2 amplification (E).

(Cat: P6887, Sigma Aldrich, USA) for 10 min and incubated in 10% buffered formalin for 10 min. The slides and probes were separately denatured, and hybridization was performed at 37°C overnight. Post-hybridization wash was done in 0.4 × SSC/0.3% NP-40 at 73°C for 3 min and slides were counterstained with DAPI.

2.4 | Reverse transcriptase PCR and Sanger sequencing

cDNA was synthesized from total RNA with random primers and Super-Script™ IV reverse transcriptase (Cat: 18,090,050, ThermoFisher, USA). PCR was performed with primers specific to *HMGA2* and *KITLG* (HMGA2-F: 5′-CAGCAGCAAGAACCAACCG; KITLG-R: 5′-CCATCC-CGGGGACATATTTGA). As quality control, *GAPDH* was also performed (GAPDH-F: 5′-AGAAGGTGGTGAAGCAGGC; GAPDH-R: 5′-TG-GGTGTCGCTGTTGAAGTC). The PCR conditions were 95°C 3 min for 1 cycle followed by 30 cycles of 95°C 30 s, 60°C 60 s, and 72°C 60 s. One microliter of the first PCR product was re-amplified with nested primers (HMGA2-Fnest: 5′-CTCCTAAGAGACCCAGGGGAA; KITLG-Rnest: 5′-AGTCACACGATTCCTGCAGAT). The PCR conditions were 95°C 3 min for 1 cycle followed by 30 cycles of 95°C 30 s, 60°C 60 s, and 72°C 60 s. The PCR product was analyzed by gel electrophoresis and Sanger sequenced.

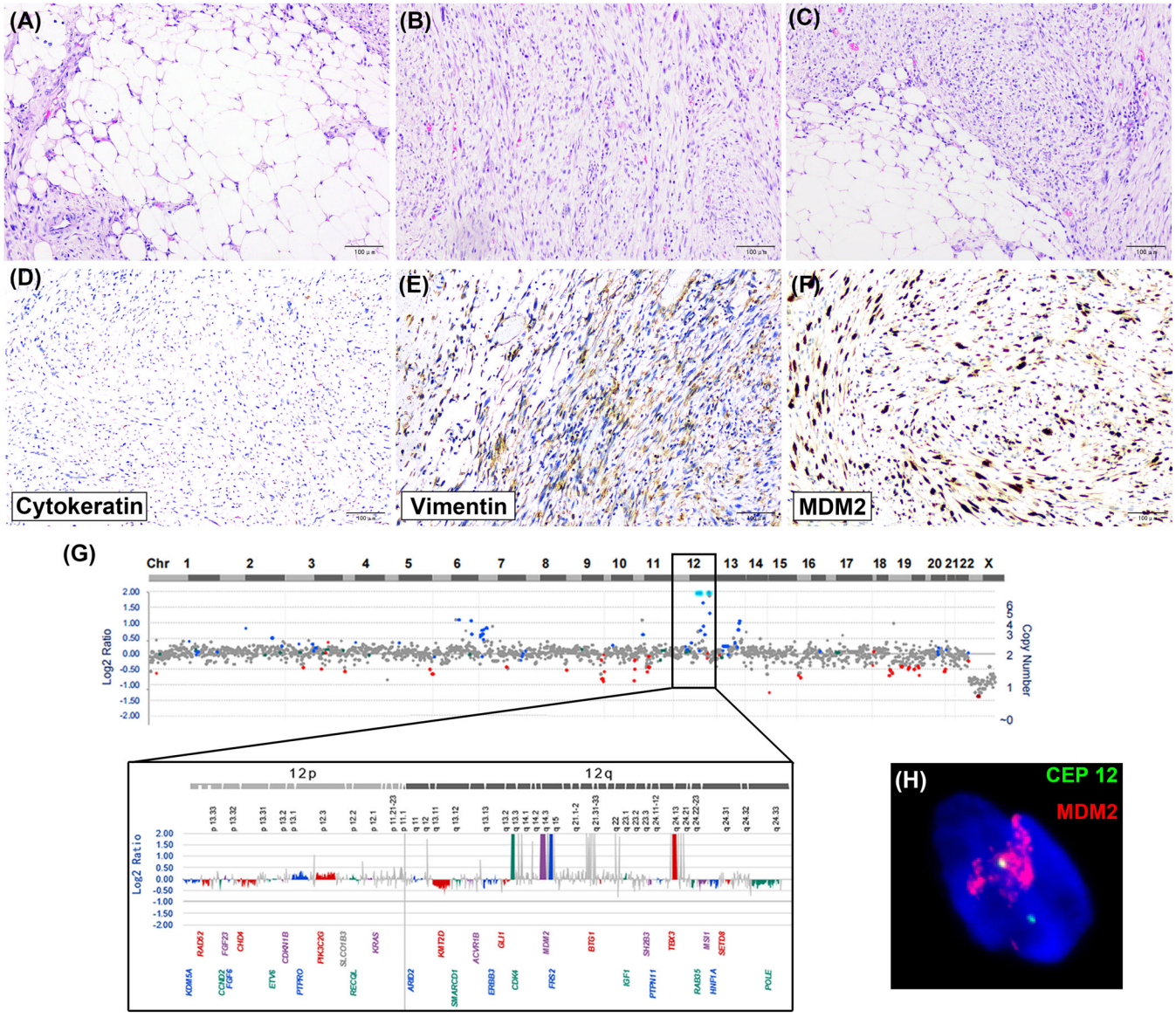

FIGURE 2 H&E staining of the relapsed tumor tissue sections showed a WDLPS component (A), a DDLPS component (B), and the transition region from WDLPS to DDLPS (C); IHC was negative for Cytokeratin (D), positive for Vimentin (E), and positive for MDM2 (F); A targeted DNA NGS assay showed complex structural alterations of chromosome 12q, leading to the amplification of *CDK4* (12q14.1) and *MDM2* (12q15). Note that *HMGA2* was not included in this DNA NGS panel (G); FISH with CEP 12 (green) and *MDM2* (red) probes showed *MDM2* amplification (H).

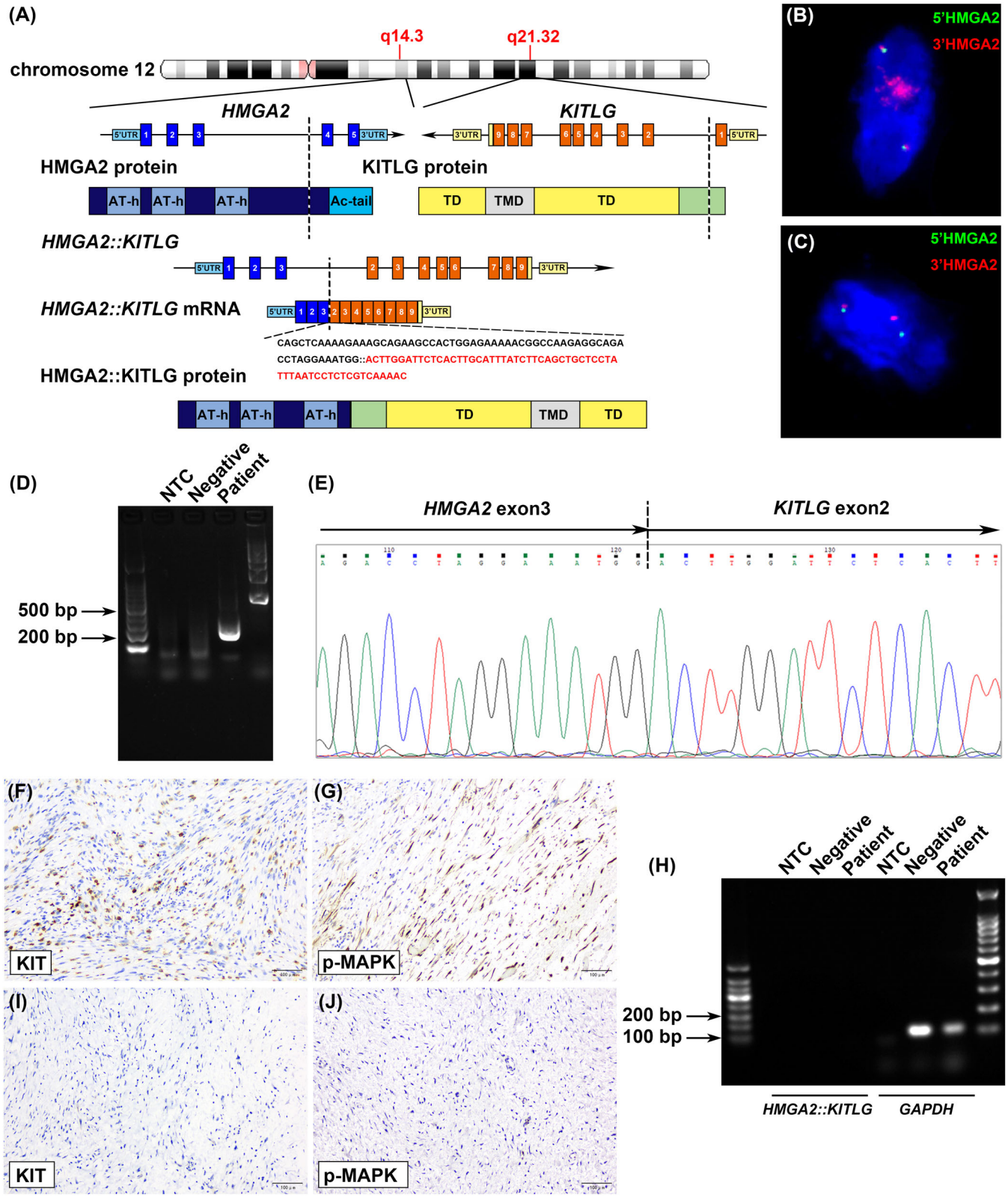

FIGURE 3 Targeted RNA NGS showed an in-frame fusion between *HMGA2* exon 3 and *KITLG* exon 2, likely resulting from an intrachromosomal 12q inversion. The main functional domains and exon position are illustrated. The location of the breakpoints was marked by dotted lines. AT-h, AT hook domain; Ac-tail, acidic terminal tail; TMD, transmembrane domain; TD, topological domain (A); FISH with a HMGA2 split-apart probe showed the amplification of 3′HMGA2 (red) in DDLPS area (B) but not in WDLPS area (C); RT-PCR with primers specific for *HMGA2* and *KITLG* amplified a fusion product at expected size in the relapsed tumor (D) but not in the primary tumor (H). NTC, no template control; Sanger sequencing of the PCR product confirmed the *HMGA2*::*KITLG* fusion (E). IHC showed a positive stain for KIT and phosphorylated MAPK in the relapsed DDLPS (F and G) but not in the primary tumor (I and J). p-MAPK, phosphorylated MAPK.

3 | RESULTS

A 55-year-old male patient underwent surgical resection of a mass measuring up to 9 cm in maximum diameter located in the lower left abdomen 3 years ago. Hematoxylin and eosin (H&E) staining of the tumor sections revealed a spindle and pleomorphic tumor, which tested positive for Vimentin and MDM2 but negative for Cytokeratin (Figure 1A–D). FISH analysis confirmed *MDM2* amplification (Figure 1E), consistent with the diagnosis of DDLPS. No WDLPS component was evident, although the tumor sample was limited. The patient was stable until recent development of abdominal distension. A CT scan revealed multiple masses in the abdominal pelvic mesentery, with the largest measuring 12.9 × 12.1 × 12.2 cm. H&E staining of the tumor biopsy showed two components, including a well-differentiated lipomatous tumor and a dedifferentiated pleomorphic spindle non-lipogenic area (Figure 2A–C). Immunohistochemistry (IHC) of tumor cells was positive for Vimentin and MDM2 and negative for Cytokeratin, both in well-differentiated area (Figure S1A–C) and dedifferentiated area (Figure 2D–F), confirming the diagnosis of relapsed DDLPS. To identify potential therapeutic interventions, targeted DNA NGS and RNA NGS were performed. DNA NGS analysis of 638 tumor-related genes, coupled with a whole-genome SNP probe set, revealed a complex structural rearrangement of chromosome 12q, resulting in the amplification of 12q14.1 → q15, encompassing *CDK4* (CN = 13), *FRS2* (CN = 11), and *MDM2* (CN = 14), along with 12q24.21, featuring *TBX3* amplification (CN = 18; Figure 2G). Additionally, a loss at 9q34.3 was identified. No other somatic mutations were detected. The *MDM2* amplification was subsequently confirmed by FISH assay (Figure 2H). Targeted RNA NGS using "bait" probes for 99 fusion genes (Table S1) detected an in-frame fusion transcript containing *HMGA2* and *KITLG*. The *HMGA2::KITLG* fusion includes the first three exons of *HMGA2* and the last eight exons of *KITLG* and is reading-frame intact (Figure 3A). The opposite transcriptional orientation of these genes on chromosome 12 suggests that the fusion event was likely caused by an intrachromosomal inversion. FISH with *HMGA2* split-apart probe showed 3′ *HMGA2* amplification but not 5′ *HMGA2* in the DDLPS area, consistent with an unbalanced *HMGA2* rearrangement with a genomic breakpoint between 5′ *HMGA2* and 3′ *HMGA2* (Figure 3B). In contrast, the WDLPS area did not exhibit 3′ HMGA2 amplification (Figure 3C). The *HMGA2::KITLG* fusion was further confirmed by reverse transcriptase PCR (RT-PCR) assay with primers specific to *HMGA2* and *KITLG* and Sanger sequencing of the PCR product (Figure 3D,E). The predicted HMGA2::KITLG chimeric protein contains three AT-hook DNA binding domains (AT-h) from HMGA2 and almost the entire KITLG, including its intact topological domains and transmembrane domain (Figure 3A). KITLG, also known as the stem cell factor, is the primary ligand for KIT, which induces KIT dimerization, autophosphorylation, and downstream signaling. IHC assays showed KIT expression and MAPK phosphorylation in tumor cells of DDLPS area (Figure 3F,G), indicating constitutive KIT activation. Differently, KIT expression and MAPK phosphorylation were not observed in WDLPS area (Figure S1D,E). In a retrospective evaluation of the primary tumor, *HMGA2* rearrangement was not detected by RT-PCR (Figure 3H), and IHC analysis did not reveal KIT expression or MAPK phosphorylation (Figure 3I,J). A summary of the molecular and IHC findings in the primary tumor and both components of the relapsed tumor is presented in Table 1. These findings suggest that the *HMGA2::KITLG* fusion was a secondary change that occurred during tumor relapse.

The patient received a chemotherapy regimen consisting of Epirubicin and Cyclophosphamide intravenously every 2 weeks for a total of four treatments. Following this, Palbociclib, a CDK4/6 inhibitor, was given as maintenance therapy. Additionally, palliative cytoreduction surgery was performed to alleviate the patient's unbearable abdominal distension. Unfortunately, despite these interventions, the patient responded poorly and ultimately succumbed to the disease 4 months after relapse.

TABLE 1 Summary of molecular and IHC results in primary and relapsed tumors.

Methods and markers		Results		
			Relapsed tumor	
		Primary tumor	WDLPS	DDLPS
NGS	DNA NGS	/	*MDM2* and *CDK4* co-amplification	
	RNA NGS	/	*HMGA2::KITLG*	
RT-PCR	*HMGA2::KITLG*	−	+	
FISH	3′*HMGA2* amplification	−	−	+
	MDM2 amplification	+	+	+
IHC	Cytokeratin	−	−	−
	Vimentin	+	+	+
	MDM2	+	+	+
	KIT	−	−	+
	p-MAPK	−	−	+

Abbreviations: DDLPS, dedifferentiated liposarcoma; FISH, fluorescence in situ hybridization; IHC, immunohistochemistry; NGS, next-generation sequencing; p-MAPK, phosphorylated MAPK; RT-PCR, reverse transcriptase PCR; WDLPS, well-differentiated liposarcoma.

4 | DISCUSSION

HMGA2 is a non-histone architectural DNA binding protein that regulates chromatin structure and gene expression. Substantial evidence shows that HMGA2 plays a critical role in several pathways crucial to tumorigenesis. For example, HMGA2 promotes cell cycle progression by increasing the expression of cell cyclins, which leads to phosphorylation of pRB and release of E2F, allowing cells to enter S phase.[4] Additionally, HMGA2 downregulates the expression of CDKN1A and CDKN2A/B,[5] two cyclin-dependent kinase inhibitors that are important for arresting the cell cycle at the S phase. HMGA2 also upregulates CCNB1 to help with the G2-M transition.[6] HMGA2 promotes stemness and epithelial-mesenchymal transition (EMT) by upregulating genes in the TGF-β/Smads pathway.[7] Several studies have linked drug resistance to HMGA2, including resistance to Sunitinib, a tyrosine kinase inhibitor, through the HMGA2-induced EMT, and resistance to gemcitabine by the HMGA2-dependent histone acetyltransferase (HAT) expression.[8,9] *HMGA2* overexpression has been observed in many tumors, including both solid tumors and leukemia, and is associated with poor prognosis. However, genomic alterations of *HMGA2* are mostly observed in mesenchymal tumors. *HMGA2* is co-amplified with *MDM2* in DDLPS, and it is believed that the collaboration between MDM2 and HMGA2 contributes to the ubiquitination and degradation of p53.[3] *HMGA2* rearrangement is mainly observed in a variety of benign mesenchymal tumors, including lipoma, leiomyoma, pulmonary chondroid hamartoma, and chondroma. *HMGA2* rearrangement can involve a breakpoint several hundred kilobases away from the gene, resulting in local chromatin structure changes that lead to *HMGA2* overexpression. Other rearrangements occur at the 3′ untranslated region (3′UTR) of *HMGA2*, where lethal-7 (*let-7*) binds. *let-7* is a noncoding miRNA that negatively regulates *HMGA2* by RNA silencing.[10] Intragenic *HMGA2* rearrangement leads to the fusion between the 3 AT-hook domains of the HMGA2 and various fusion partner genes. The recurrent nature of *HMGA2* fusion genes highlights the significant contribution of fusion partners to oncogenesis. For example, in *HMGA2*::*LLP*, occurring in approximately 1/3 of lipomas, both the N-terminal HMGA2 and the C-terminal LPP sequences are required for the transactivation of the *Col11a2* promoter.[11]

KITLG is the primary ligand for KIT and is essential for spermatogenesis, hematopoiesis, and melanocytes. During early embryonic development, KITLG functions as a crucial chemokine that facilitates germ cell migration.[12] Perturbations in this signaling pathway can lead to the development of germ cell tumors. In a recent case study, we reported a 3-year-old girl who had simultaneous germ cell tumor and mastocytosis. Genomic profiling of both tumors revealed an identical *KIT* activation mutation, which supports the essential role of KITLG/KIT signaling in both germ cell migration and hematopoiesis.[13] While genomic alterations of *KITLG* have not been reported, *KIT* mutations and rearrangements that lead to constitutive activation of the kinase domain have been observed in gastrointestinal stromal tumors, mastocytosis, and melanoma.

The oncogenic mechanism underlying HMGA2::KITLG likely involves the constitutive activation of KIT signaling. The *HMGA2* rearrangement leads to the loss of the *let-7* binding site, which can result in overexpression of the *HMGA2*::*KITLG* fusion transcript. The HMGA2::KITLG fusion contains almost the entire KITLG coding sequence and is likely able to bind to KIT, leading to its activation. This hypothesis is supported by the detection of KIT expression in tumor cells and activated MAPK, a major downstream signaling molecule, by IHC. This scenario has potential therapeutic implications, as KIT kinase inhibitors are widely available in the clinic. Unfortunately, our patient's disease progressed rapidly, and anti-KIT therapy was not feasible. Alternatively, *HMGA2*::*KITLG* may be a fortuitous secondary rearrangement, resulting from chromosome 12 chromothripsis or inevitable chromosome instability via the breakage-fusion-bridge cycle, a characteristic feature of this tumor with a ring chromosome 12. Intriguingly, KIT expression was observed in 30% of DDLPS, while it remained unexpressed in the WDLPS component.[14] Nevertheless, the role of KIT signaling in the progression of WDLPS/DDLPS warrants further investigation and evaluation.

FUNDING STATEMENT

This work was supported by the 2022 Central South University Postgraduate Teaching Case Database Construction Project (2022ALK039).

CONFLICT OF INTEREST STATEMENT

The authors declare that they have no conflict of interest with the contents of this article.

DATA AVAILABILITY STATEMENT

The data that support the findings of this study are available from the corresponding author upon reasonable request.

REFERENCES

1. Bartuma H, Panagopoulos I, Collin A, et al. Expression levels of HMGA2 in adipocytic tumors correlate with morphologic and cytogenetic subgroups. *Mol Cancer*. 2009;8:36.
2. Necchi A, Basile G, Pederzoli F, et al. Primary adult retroperitoneal sarcoma: a comprehensive genomic profiling study. *Soc Int Urol J*. 2021;2(4):216-228.
3. Wang Y, Hu L, Wang J, et al. HMGA2 promotes intestinal tumorigenesis by facilitating MDM2-mediated ubiquitination and degradation of p53. *J Pathol*. 2018;246(4):508-518.
4. Mansoori B, Mohammadi A, Ditzel HJ, et al. HMGA2 as a critical regulator in cancer development. *Genes (Basel)*. 2021;12(2):269.
5. Markowski DN, von Ahsen I, Nezhad MH, Wosniok W, Helmke BM, Bullerdiek J. HMGA2 and the p19Arf-TP53-CDKN1A axis: a delicate balance in the growth of uterine leiomyomas. *Genes Chromosomes Cancer*. 2010;49(8):661-668.
6. Arora S, Singh P, Rahmani AH, Almatroodi SA, Dohare R, Syed MA. Unravelling the role of miR-20b-5p, CCNB1, HMGA2 and E2F7 in development and progression of non-small cell lung cancer (NSCLC). *Biology*. 2020;9(8):201.
7. Hou M, Bao X, Luo F, Chen X, Liu L, Wu M. HMGA2 modulates the TGFbeta/Smad, TGFbeta/ERK and notch signaling pathways in

human lens epithelial-mesenchymal transition. *Curr Mol Med*. 2018; 18(2):71-82.
8. Marijon H, Dokmak S, Paradis V, et al. Epithelial-to-mesenchymal transition and acquired resistance to sunitinib in a patient with hepatocellular carcinoma. *J Hepatol*. 2011;54(5):1073-1078.
9. Dangi-Garimella S, Sahai V, Ebine K, Kumar K, Munshi HG. Three-dimensional collagen I promotes gemcitabine resistance in vitro in pancreatic cancer cells through HMGA2-dependent histone acetyltransferase expression. *PLoS One*. 2013;8(5):e64566.
10. Lee YS, Dutta A. The tumor suppressor microRNA let-7 represses the HMGA2 oncogene. *Genes Dev*. 2007;21(9):1025-1030.
11. Kubo T, Matsui Y, Goto T, Yukata K, Yasui N. Overexpression of HMGA2-LPP fusion transcripts promotes expression of the alpha 2 type XI collagen gene. *Biochem Biophys Res Commun*. 2006;340(2): 476-481.
12. Gu Y, Runyan C, Shoemaker A, Surani MA, Wylie C. Membrane-bound steel factor maintains a high local concentration for mouse primordial germ cell motility, and defines the region of their migration. *PLoS One*. 2011;6(10):e25984.
13. Xiao P, Chen P, Lang X, et al. Ovarian germ cell tumor/mastocytosis with KIT mutation: a unique clinicopathological entity. *Genes Chromosomes Cancer*. 2022;61(1):50-54.
14. Tayal S, Classen E, Bemis L, Robinson WA. C-kit expression in dedifferentiated and well-differentiated liposarcomas; immunohistochemistry and genetic analysis. *Anticancer Res*. 2005;25(3B):2215-2220.

SUPPORTING INFORMATION

Additional supporting information can be found online in the Supporting Information section at the end of this article.

How to cite this article: Zhou S, Zhang C, Zhang Z, et al. A novel *HMGA2::KITLG* fusion in a dedifferentiated liposarcoma with amplification of *MDM2* and *HMGA2*. *Genes Chromosomes Cancer*. 2023;1-7. doi:10.1002/gcc.23200